Depth-resolved low-coherence enhanced backscattering

Young L. Kim, Yang Liu, Vladimir M. Turzhitsky, Ramesh K. Wali, Hemant K. Roy, and Vadim Backman

Department of Biomedical Engineering, Department of Gastroenterology, Northwestern University, Evanston, Illinois 60208

Received October 27, 2004

The phenomenon of enhanced backscattering (also known as coherent backscattering), an object of substantial scientific interest, has awaited application to tissue optics for the past two decades. Here we demonstrate, for the first time to our knowledge, depth-resolved spectroscopic elastic light scattering measurements in tissue by use of low-coherence enhanced backscattering (LEBS). We achieve the depth resolution by exploiting the nature of the LEBS peak that contains information about a wide range of tissue depths. We further demonstrate that depth-resolved LEBS spectroscopy has the potential to identify the origin of precancerous transformations in the colon at an early, previously undetectable stage. © 2005 Optical Society of America

OCIS codes: 030.1670, 290.1350, 300.6170, 170.4580.

Enhanced backscattering (EBS), otherwise known as coherent backscattering, is a spectacular manifestation of self-interference effects in elastic light scattering, which leads to an enhanced scattered intensity in the backward direction. EBS originates from the constructive interference between a wave traveling a multiple-scattering path and its reciprocal counterpart following a time-reversed path. EBS has been observed in a variety of systems ranging from paint to biological tissue.[1–6] Although the EBS phenomenon in nonbiological media has attracted significant research interest, it has been extremely difficult to investigate EBS in biological tissue because of extremely narrow peaks [its angular FWHM is $w \approx \lambda/(3\pi l_s^*) \sim 0.005°$, where λ is the wavelength of the light and l_s^* is the transport mean free path] and excessive speckle. Experimental observation of such an extremely narrow EBS peak has only recently been achieved in pioneering experiments by Sapienza *et al.*[5] Furthermore, conventional EBS measurements could provide neither depth-resolved nor spectroscopic information about optical properties of tissue. Recently, we developed low-coherence enhanced backscattering (LEBS) spectroscopy that overcomes the major barriers that have so far impeded the use of this fascinating phenomenon in biological applications. LEBS combines broadband ($400\ \text{nm} < \lambda < 700\ \text{nm}$), low spatial coherence (coherence length $L_c \ll l_s^*$) illumination and spectrally resolved, low temporal coherence detection, giving rise to EBS peaks that are broadened by more than 2 orders of magnitude ($w \approx 0.5°$) and are speckle free. These peaks can be recorded as a function of wavelength.[6]

It is widely recognized that depth resolution is of paramount importance to furthering the capabilities of diagnostic tissue spectroscopy. In particular, selective probing of the mucosa and the epithelium (the superficial tissue lining the inner surfaces of the body) is crucial for early cancer detection owing to the fact that nearly 90% of human cancers originate from the epithelium. In this Letter we present what is to our knowledge the first implementation of LEBS spectroscopy to achieve depth-resolved measurements of elastic light scattering spectra. Furthermore, we show that by selectively probing tissue depths at which the precancerous transformations originate, LEBS spectroscopy permits diagnosis of the earliest stage of colonic neoplasia, which currently cannot be detected by histological examination of biopsy specimens or molecular and genetic tests.

In LEBS, depth resolution can be achieved by two complementary means. First, low spatial coherence illumination separates low-order scattering from diffused multiple scattering by preventing long-traveling waves from interfering with each other.[6] Only photons emerging from tissue at a distance of $r < \sim L_c$ from their point of incidence can contribute to LEBS, which limits the depth of penetration of LEBS photons. Second, within the maximum penetration depth determined by L_c, depth resolution can be further achieved by analysis of the angular profile of an EBS peak $I_{\text{EBS}}(\theta, \lambda)$ that contains information about a wide range of tissue depths.[2,3] $I_{\text{EBS}}(q)$ is the Fourier transform of its radial intensity distribution $P(r)$: $I_{\text{EBS}}(q) = \int P(r)\exp(iqr)\mathrm{d}r$, where $q = 2\pi\theta/\lambda$ and $P(r) \equiv rp(r)$, with $p(r)$ being the probability of photons to emerge from the surface at a radial distance r.[1] Thus short light paths mainly give rise to the periphery of an EBS peak, whereas longer light paths give rise to EBS at smaller angles θ (i.e., closer to the backscattering direction). Moreover, the Fourier transform relationship provides an effective method to obtain $P(r)$ from EBS measurements. It is well known that the depth of penetration of photons generating $P(r)$ is related to r. Therefore depth-resolved measurements can be achieved by either sampling $I_{EBS}(\theta)$ at different θ within a single EBS peak or sampling $P(r)$ at different r. Thus LEBS spectroscopy opens up the possibility of performing spectroscopic measurements at any given depth.

The LEBS instrument used to demonstrate the depth-resolution capabilities of LEBS was described elsewhere.[6] In brief, a beam of broadband cw light from a 500-W xenon lamp was collimated, polarized, and delivered onto a sample at a 15° angle of inci-

0146-9592/05/070741-3/$15.00

dence to prevent the collection of specular reflection. The light backscattered by a sample was collected by an analyzing polarizer oriented along the polarization of the incident light, a lens, and an imaging spectrograph positioned in the focal plane of the lens and coupled to a CCD camera. The lens projected the angular distribution of the backscattered light onto the slit of the spectrograph, which, in turn, dispersed this light according to its wavelength in the direction perpendicular to the slit. Thus the CCD recorded a matrix of light-scattering intensity as a function of wavelength ($\lambda = 400-700$ nm) and backscattering angle ($\theta = -7° - 7°$) simultaneously. The spatial coherence length of illumination and the temporal coherence length of detection were 140 and 30 μm, respectively. The EBS peaks were normalized such that $I_{\mathrm{EBS}}(\theta,\lambda) = [I(\theta,\lambda) - I_{\mathrm{BASE}}(\lambda)]/I_{\mathrm{REF}}(\lambda)$, where I_{BASE} is the baseline (incoherent) intensity measured at large angles ($\theta > 3°$) and I_{REF} is the reference intensity collected from a reflectance standard.

As an illustration of LEBS, Fig. 1(a) shows a typical LEBS peak $I_{\mathrm{EBS}}(\theta,\lambda)$ recorded from *ex vivo* rat colon tissue. The unique features of LEBS that permit its observation in biological tissue are evident: The peak is broadened by 2 orders of magnitude ($w \approx 0.5°$), speckle free, and recorded as a function of λ. Figure 1(b) shows $P(r,\lambda)$ obtained from $I_{\mathrm{EBS}}(\theta,\lambda)$. We point out that previously it was extremely difficult to obtain $P(r)$ for small r ($r < \sim 300$ μm) directly.[7]

We investigated the depth resolution of LEBS using physical tissue models consisting of aqueous suspensions of polystyrene microspheres of various diameters from 0.24 to 0.5 μm (Duke Scientific). We measured the angular profiles of EBS peaks by varying mean free path l_s from 52 to 300 μm and l_s^* from 195 to 1131 μm (l_s and l_s^* were calculated using Mie theory and confirmed by integrating sphere measurements). The optical properties of the tissue models were within the tissue optics range. For each set of optical parameters, physical thickness T of the tissue models was varied from 0 to 160 μm with a 9-μm step and signals $I_{\mathrm{EBS}}(\theta,\lambda;T)$ were obtained. Varying T provides a simple method for quantifying the contribution of different depths to the EBS signal.[3] Indeed, $I_{\mathrm{EBS}}(T) = \int_0^T C(t)\mathrm{d}t$, where $C(T)$ is the contribution of depth T to the EBS signal. Figure 2(a) shows a series of representative EBS peaks obtained for different T (with $l_s = 52$ μm, $l_s^* = 195$ μm). As T increases, EBS intensity at $\theta = 0°$ first increases, and then saturates at $T_c \sim 90$ μm, which is primarily determined by L_c. That $I_{\mathrm{EBS}}(T)$ levels off after $T_c \sim 90$ μm indicates that the EBS signal is determined by $T < T_c$ and deeper scatterers do not contribute to the EBS signal. We defined the EBS penetration depth at scattering angle θ, $L_p(\theta)$, as T such that $I_{\mathrm{EBS}}(T = L_p)$ reaches 90% of its saturation value, as shown in Fig. 2(b). As illustrated in Figs. 2(c) and 2(d), an analogous analysis of $P(r,T)$ allowed us to determine the penetration depth $L_p(r)$as a function of r.

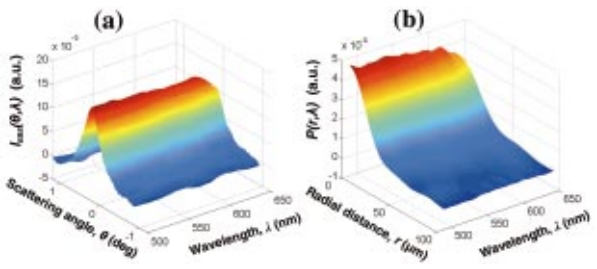

Fig. 1. (a) EBS intensity $I_{\mathrm{EBS}}(\theta,\lambda)$ obtained from *ex vivo* rat colon tissue with the LEBS spectroscopy instrument. (b) Radial intensity distribution $P(r,\lambda)$ obtained from the inverse Fourier transform of $I_{\mathrm{EBS}}(\theta,\lambda)$.

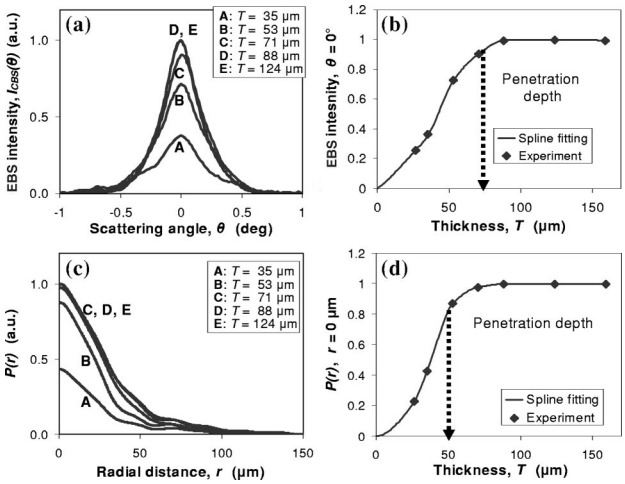

Fig. 2. (a) EBS intensity $I_{\mathrm{EBS}}(\theta)$ recorded from a typical tissue model ($l_s = 52$ μm and $l_s^* = 195$ μm) for $T = 35-124$ μm. (b) $I_{\mathrm{EBS}}(\theta = 0°)$ as a function of T. Penetration depth $L_p(\theta = 0°)$ is defined as T for which $I_{\mathrm{EBS}}(\theta = 0°)$ reaches 90% of its saturated value. (c) Radial intensity distribution $P(r)$ obtained for $T = 35-124$ μm. (d) $P(r = 0)$ as a function of T.

Figures 3(a) and 3(b) show LEBS penetration depths $L_p(\theta)$ and $L_p(r)$ for different optical properties of the tissue models. As expected, a small angle θ corresponds to deeper penetration depths, whereas a large θ corresponds to shorter depths, and $L_p(\theta)$ decreases with θ as shown in Fig. 3(a). Figure 3(b) shows that $L_p(r)$ increases with r, thus supporting the concept that greater separation between illumination and detection points enables one to probe deeper tissue depths. As shown in Figs. 3(a) and 3(b), tissue depths from ~ 40 μm (approximately a single cell layer) to ~ 100 μm (the thickness of the entire mucosa of most biological tissues) can be selectively assessed by means of selecting appropriate θ or r. Importantly, L_p does not depend strongly on the optical properties of the tissue, and thus the wavelength of light (for l_s and l_s^* relevant to tissue optics), and is primarily determined by θ or r (for $r < l_s$). These results demonstrate that depth-resolved measurements can be achieved either by sampling $I_{\mathrm{EBS}}(\theta)$ at different angles or $P(r)$ at different radial distances.

As discussed above, depth-resolved spectroscopic measurements are exceedingly useful for tissue characterization and diagnosis. Because the epithelial cells are the first affected in carcinogenesis, diagnos-

tic information must be obtained from the most superficial tissue. Furthermore, the depth-dependent biological heterogeneity of the colonic epithelium underscores the need to selectively assess the epithelial cells at different depths. The major unit of organization of the colonic mucosa is the crypt. Epithelial cells at the base of the crypt (~70 μm below tissue surface) are capable of proliferation, whereas epithelial cells at the top of the crypt (~30 μm) undergo apoptosis. Moreover, the importance of the depth resolution of EBS is underlined by the fact that the cells that are initially involved in neoplastic transformations should be located in a specific area of the crypt.

To test the potential of depth-resolved LEBS spectroscopy for early cancer diagnosis, we performed animal studies with the azoxymethane- (AOM-) treated rat model of colon carcinogenesis, which is one of the most robust and well-tested animal models of colon carcinogenesis.[8] In AOM-treated rats, colon carcinogenesis progresses through the same steps as in humans: The earliest detectable marker of colon carcinogenesis, aberrant crypt foci, develops ~8–12 weeks after the AOM injection, adenomas are observed at 20–30 weeks, and carcinomas develop in 40 weeks. Twenty-four male Fisher 344 rats (150–200 g) (St. Charles) were randomized equally to groups that received either two weekly intraperitoneal injections of AOM (15 mg/kg) or saline. Rats were sacrificed at various time points (2, 4, and 6 weeks) after the second injection. At these early time points, no currently known histologic, molecular, or genetic markers have been able to detect preneoplastic transformation. For each animal, LEBS measurements were performed from ~50 tissue sites uniformly distributed throughout the colonic surface.

We probed the upper (~40 μm) and the lower (~70 μm) compartments of the mucosa by sampling EBS spectra $I_{\mathrm{EBS}}(\theta,\lambda)$ at θ=0.25° and θ=0°, respectively. As discussed above, the lower compartment includes the basal colonic cells, whereas the upper compartment is limited to the most superficial layer of the epithelial cells. Typically, $I_{\mathrm{EBS}}(\lambda)$ is a declining function of wavelength and its steepness depends on the size distribution of submicrometer intraepithelial structures.[9] To characterize $I_{\mathrm{EBS}}(\lambda)$ with a single parameter, we obtained linear fits to $I_{\mathrm{EBS}}(\lambda)$ using linear regression from 530 to 640 nm. The absolute

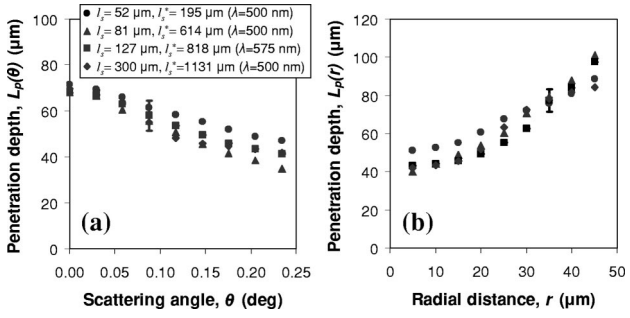

Fig. 3. (a) Penetration depth $L_p(\theta)$ as a function of θ. (b) $L_p(r)$ as a function of r. $L_p(\theta)$ decreases with θ. $L_p(r)$ increases with r.

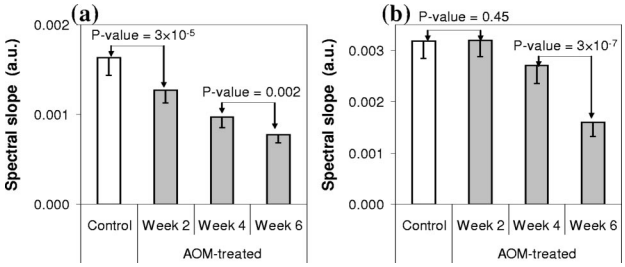

Fig. 4. Spectral slopes obtained from precancerous colonic tissues at 2, 4, and 6 weeks after the initiation of colon carcinogenesis compared with the negative control saline-treated rates: (a) lower compartment ($L_p \approx 70$ μm) and (b) upper compartment ($L_p \approx 40$ μm) of the crypts.

value of the linear coefficient of the fit is referred to as the spectral slope. Figures 4(a) and 4(b) show alterations of the spectral slope obtained from the AOM-treated rats compared with control values in the two compartments. In the lower compartment the spectral slope was dramatically decreased as early as 2 weeks after the carcinogen treatment (P value $=3\times10^{-5}$) and continued to decrease over the course of the experiment. On the other hand, in the upper compartment the spectral slope did not change at 2 weeks (P value = 0.45) but instead was dramatically altered later in the process of carcinogenesis (P value $=3\times10^{-7}$). This result is consistent with the notion that the earliest carcinogenic changes occur in the basal compartment of the mucosa and progress toward the lumenal surface. Thus alterations in the superficial cells are more diagnostic for later (although still predysplasic) stages of the disease. In summary, we demonstrate that depth-resolved spectroscopic LEBS measurements enable us to identify the location of the earliest predysplastic changes in living tissue far earlier than is currently possible with any other available diagnostic method.

This study was supported in part by National Cancer Institute grant 1R21CA102750 and National Science Foundation grant BES-0238903. We also thank A. Wax and J. F. de Boer for helpful discussions. Y. L. Kim's e-mail address is younglae@northwestern.edu.

References

1. E. Akkermans, P. E. Wolf, and R. Maynard, Phys. Rev. Lett. **56**, 1471 (1986).
2. R. Vreeker, M. P. van Albada, R. Sprik, and A. Lagendijk, Phys. Lett. A **132**, 51 (1988).
3. S. Etemad, R. Thompson, and M. J. Andrejco, Phys. Rev. Lett. **59**, 1420 (1987).
4. K. M. Yoo, G. C. Tang, and R. R. Alfano, Appl. Opt. **29**, 3237 (1990).
5. R. Sapienza, S. Mujumdar, C. Cheung, A. G. Yodh, and D. Wiersma, Phys. Rev. Lett. **92**, 033903 (2004).
6. Y. L. Kim, Y. Liu, V. M. Turzhitsky, H. K. Roy, R. K. Wali, and V. Backman, Opt. Lett. **29**, 1906 (2004).
7. M. Dogariu and T. Asakura, Waves Random Media **4**, 429 (1994).
8. M. Kobaek-Larsen, I. Thorup, A. Diederichsen, C. Fenger, and M. R. Hoitinga, Comp. Med. East West **50**, 16 (2000).
9. H. K. Roy, Y. Liu, R. K. Wali, Y. L. Kim, A. K. Kromin, M. J. Goldberg, and V. Backman, Gastroenterology **126**, 1071 (2004).